Junction recombination current in abrupt junction diodes

Author:

Corkish, Richard Paul; Green, Martin A.

Junction recombination current in abrupt junction diodes under forward bias

Richard Corkish[a] and Martin A. Green[b]
Centre for Photovoltaic Devices and Systems, University of New South Wales, Sydney 2052, Australia

A new, analytical method is presented for calculating the depletion-region recombination current for abrupt-junction diodes under forward bias. The method is appropriate when the recombination current is dominated by recombination through Shockley–Read–Hall centers at a single energy level whose density does not vary strongly with position through the device. The new model is systematically compared with earlier models and with the results of finite-element analyses using PC-1D. If it is reasonably assumed that PC-1D is the most accurate of the methods considered here, the others may be ranked according to their proximity to the PC-1D result. It is shown that the new method, despite its simplicity, yields results closer to PC-1D than the earlier models for many practical situations. In addition, it is shown that one existing model may be brought into agreement with the finite-element analysis by a simple modification of the limits of integration. © *1996 American Institute of Physics.* [S0021-8979(96)07216-7]

I. INTRODUCTION

Sah, Noyce, and Shockley[1] (SNS) presented in 1957 the first comprehensive theory for modelling carrier generation and recombination in the space-charge region of a *p-n* junction and their expression[2] for the generation-recombination current under small forward bias remains in common use. In that work the doping density on each side of the junction was assumed equal. Choo[3] extended the SNS theory to include asymmetrically doped devices and the resulting expression[4] for the current under small forward bias is also frequently cited. However, although those treatments[1,3] are the most heavily cited in this area, neither gives good agreement, in general, with more precise calculations. In each of these models there is assumed to be a uniformly distributed set of Shockley–Read–Hall (SRH) generation-recombination centers at a single energy level within the band gap. The recombination rate in steady state is given by[5]

$$U(x) = [n(x)p(x) - n_i^2]\{\tau_{n0}[p(x) + p_1] + \tau_{p0}[n(x) + n_1]\}^{-1}, \quad (1)$$

where n_i is the intrinsic carrier concentration, τ_{n0}, τ_{p0} are (excess) carrier lifetime parameters[6] dependent on the capture cross section and density of the centers,

$$n_1 = n_i \exp[(E_t - E_i)/kT], \quad p_1 = n_i \exp[(E_i - E_t)/kT] \quad (2)$$

are the carrier concentrations if the Fermi level were to lie at E_t, the energy level of the recombination centers, and E_i is the intrinsic energy level. The recombination rate is a function of position due to the variation of the carrier concentrations with distance but the lifetime parameters are assumed to be independent of position. The generation-recombination

current contribution from the space-charge region is found by integrating the recombination rate over this region:

$$J_{rg} = q \int U \, dx \quad (3)$$

and the limits of integration are the boundaries of the space-charge region (SCR). According to the depletion approximation,[7] these boundaries are given by

$$W_n = WN_A/(N_A + N_D), \quad W_p = WN_D/(N_A + N_D), \quad (4)$$

where N_A and N_D are the concentrations of ionized acceptor and donor dopants on the *p*- and *n*-type sides of the junction respectively, and W_p and W_n are the thicknesses of the space-charge region on the *p*- and *n*-type sides of the junction. The overall width of the SCR is given by

$$W = W_n + W_p = [2\epsilon/q(V_{bi} - V_a)(N_A^{-1} + N_D^{-1})]^{1/2}, \quad (5)$$

where V_{bi} is the built-in voltage of the junction, ϵ is semiconductor's permittivity, q is the electronic charge, and V_a is the bias voltage.

It should be noted that numerical modeling[8] has shown that the depletion approximation does not always give a good description of the extent of the SCR when the doping densities on either side of the abrupt junction are unequal. However, in the absence of a more precise definition of the SCR and in order to maintain consistency with preceding studies of SCR recombination current, we use Eq. (5) to define the SCR. In particular, the depletion approximation tends to underestimate the extent of the region on the heavily doped side within which the space charge is significant. Consequently, the boundaries described by Eq. (4) do not always enclose the entire region within which the electric field is significant and care must be exercised, when calculating overall diode currents, to appropriately model the regions beyond W_n and W_p.

In order to simplify the calculation, both SNS and Choo assumed a linear variation of electrostatic potential, $\Psi(x)$, across the space-charge region or, equivalently, assumed that the electrostatic field is constant (at its average value) across

[a]Electronic mail: r.corkish@unsw.edu.au
[b]Electronic mail: m.green@unsw.edu.au

the space-charge region. A maximum error of 50% in the field value is attributed by SNS to this approximation and we note that the generation-recombination current is inversely proportional to the field. Results derived in this work show that errors can occur which are far in excess of this level. Several attempts have been made to derive approximate analytical methods for calculating the generation-recombination current without resort to the latter assumption of average electrostatic field. Sah, Noyce, and Shockley, in their idealized model,[9] considered a symmetrical junction with equal lifetimes and recombination centers at the intrinsic Fermi level, E_i. In that case the value of the field at the junction, rather than the average value, was used to calculate the generation-recombination current. Van der Ziel[10] pointed out that for such an idealized case the integrand, U, has its maximum value, U_{max}, at the metallurgical junction and only the region close to U_{max} makes a major contribution to the current. In a more general treatment, Simeonov and Ivanovich[11] argue that the recombination rate is negligible when the potential differs from its value at U_{max}, by more than two to three times kT/q and, hence, assume a constant value of the electrostatic field equal to its value at x_m (the position at which U_{max} occurs, which is generally not at the metallurgical junction). Parikh and Lindholm,[12] in their treatment of SCR recombination in heterojunction bipolar transistors, expand the potential variation with position in a Taylor series and discard all but the linear term. Choo[13] recently modified his earlier work[3] by replacing the average field with the field at x_m. Shur[14] derived a simple approximation for the recombination current, limited to situations where the lifetimes are equal and $E_t = E_i$ and Starosel'skii[15] published a method which requires the experimental determination of two parameters.

Nussbaum[16] expressed $d\psi/dx$ analytically and avoided reliance on an assumption of a constant field value or on the depletion approximation. He was thus able to integrate (numerically) in two steps, one each side of the junction. In one sense, this solution is ''exact'' but the results disagree with the other methods considered here since the locations corresponding to these potential limits lie beyond the SCR boundaries defined by Eq. (4). The difference arises from three separate causes. Firstly, the depletion approximation does not define boundaries for the SCR where the electric field falls to zero and in most real cases the electric field is nonzero at W_n and W_p. Secondly, under forward bias there exist ohmic voltage drops across the ''bulk'' regions.[17] Finally, as discussed above, the depletion approximation is not always a good description of the SCR when the doping densities on either side of the junction differ significantly.[8] In Appendix A we give an alternative derivation for Nussbaum's method. We also show that if the limits of integration are changed to $\psi = 0.3kT$ and $\psi = V_{bi} - V_a - 0.3kT$, then we obtain excellent agreement with values derived from PC-1D using the spatial limits of Eq. (4).

In this work we first calculate, using the PC-1D finite element analysis package,[18] and discuss the form of the recombination rate versus position function, $U(x)$, as it depends on asymmetries in the carrier lifetimes and doping densities. In Sec. III we introduce a new analytical method to
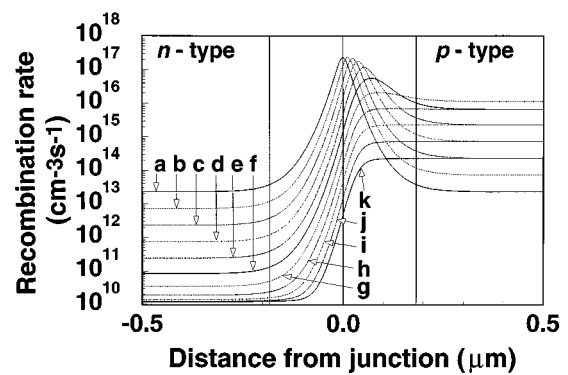

FIG. 1. Shockley–Read–Hall recombination rate as a function of distance perpendicular to an abrupt, symmetrically doped (10^{16} cm^{-3}) Si p-n junction. Trap energy is equal to the intrinsic energy and the forward bias is 0.2 V. The product of the lifetime parameters, $\tau_{p0}\tau_{n0}$, is set to 10^{-12} s^2 and the parameter for the different curves is their ratio, τ_{p0}/τ_{n0}. Values for that ratio are: (a) 1, (b) 10, (c) 10^2, (d) 10^3, (e) 10^4, (f) 10^5, (g) 10^6, (h) 10^7, (i) 10^8, (j) 10^9, (k) 10^{10}. The vertical lines are the positions of the junction and the boundaries of the depletion region.

obtain an approximation to the recombination current in abrupt junctions under forward bias. Our techniques for modelling space-charge recombination using PC-1D are described in Sec. IV and in the following section we compare our new method with PC-1D and with other analytical methods from the literature. All calculations assume a temperature of 300 K. We ignore the contribution to the recombination current of trap-assisted tunneling.[19] Preliminary reports of this work have appeared elsewhere.[20,21]

II. FORM OF $U(x)$ WITH LIFETIME AND DOPING ASYMMETRIES

A. Lifetime asymmetry

Figure 1 shows the recombination rate as a function of position as predicted for a 1-μm-thick, symmetrically doped ($N_A = N_D = 10^{16}$ cm^{-3}) silicon diode with $E_t = E_i$ by the finite element program, PC-1D. For each curve, the forward bias has been set to 0.2 V and the parameter for the set of curves is the ratio of the (excess) carrier lifetime parameters, τ_{p0}/τ_{n0}. The product of the lifetimes is held constant at 1×10^{-12} s^2. For equal lifetimes the recombination rate is strongly peaked at the location of the metallurgical junction and declines towards the same constant value in each bulk region. Changing the τ_{p0}/τ_{n0} ratio moves the peak in the recombination rate towards the side in which the minority carrier lifetime is shorter. In our example, an increase in τ_{p0}/τ_{n0} causes more recombination to occur on the p-type side of the junction than on the n-type side. The peak in the recombination rate eventually moves outside the depletion region (as defined by the depletion approximation) and becomes less prominent. For these cases of very great asymmetry in the lifetimes, the recombination rate across approximately 30% of the SCR adjoining the bulk region with low minority-carrier lifetime is essentially the same as the rate in that bulk region. Ideality factors can approach unity for large values of lifetime asymmetry.[22] For these cases, the useful-

ness of separating the recombination into bulk and SCR components is open to question. It is also worth noting that since the bulk thickness will usually greatly exceed that of the SCR the SCR recombination current will usually be negligible in comparison to bulk current when electron and hole lifetimes differ by several orders of magnitude.

For each curve in which a peak is clearly evident in Fig. 1, there is some ''spillover'' of enhanced recombination rate from the SCR into each bulk region. When the asymmetry is small, this spillover is unimportant since only an insignificant fraction of the total recombination current would be neglected if the limits of the integral in Eq. (3) are set to the SCR edges given by the depletion approximation.[1,3] However, a significant fraction of the recombination current may not be accounted for in cases like some of those shown in Fig. 1 (see, for example, the curve corresponding to $\tau_{p0}/\tau_{n0}=10^6$) in which the spillover excess recombination rate approaches the peak value in the SCR. Nussbaum's theory, without modification of the limits of integration, includes all the spillover recombination as well as the bulk recombination on both sides of the junction up to the points where the potential ceases to vary with distance.

B. Doping asymmetry

We also used PC-1D to model the effect of doping asymmetry on the form of $U(x)$. Figure 2(a) shows the effect of increasing N_D while keeping N_A fixed at 10^{14} cm^{-3} and Fig. 2(b) has the results of reducing N_A, while N_D is fixed at 10^{18} cm^{-3}. The peak in the recombination rate moves away from the more heavily doped side of the junction but in each case the peak is contained well within the boundaries of the SCR.

III. NEW APPROXIMATION FOR RECOMBINATION CURRENT

In this section we present a new approach to the estimation of recombination current in abrupt p-n junctions under forward bias. The theory applies directly to situations in which the maximum value of $U(x)$ occurs on the p-type side of the abrupt junction and extension of the theory to the n-type side is straightforward.

A. Cases where $U(x)$ strongly peaked

Assuming constant quasi-Fermi levels across the depletion region and in the neutral bulk for the respective majority carrier,[23] we have

$$np = n_i^2 \exp[qV_a/(kT)], \tag{6}$$

where V_a is the potential between the contacts. This allows p to be eliminated as a variable from Eq. (1) and the electron
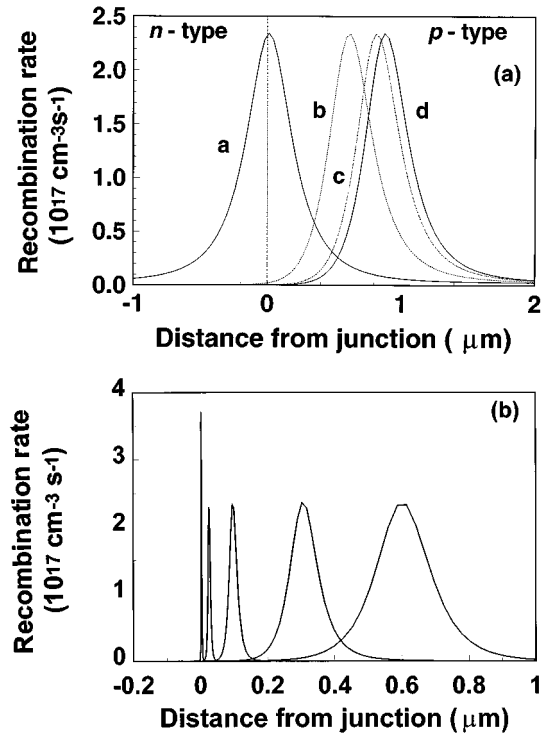

FIG. 2. Effect of doping asymmetry on the Shockley–Read–Hall recombination rate as a function of distance perpendicular to an abrupt Si p-n junction when the doping is varied on (a) the side of the junction opposite that on which the recombination rate is maximum and (b) on the same side. Trap energy is equal to the intrinsic energy, the forward bias is 0.2 V and $\tau_{p0} = \tau_{n0} = 10^{-6}$ s. In (a) the acceptor doping level is maintained equal to 10^{14} cm^{-3}, while the donor doping is set to (a) 10^{14}, (b) 10^{15}, (c) 10^{16}, (d) 10^{17} cm^{-3}. In (b) the donor doping is fixed at 10^{18} cm^{-3} and the five peaks, from left to right, correspond to acceptor concentrations of 10^{18}, 10^{17}, 10^{16}, 10^{15}, and 10^{14} cm^{-3}.

and hole concentrations at which the recombination rate is maximum to be found by differentiation of the denominator:

$$n(x_m) = (\tau_{n0}/\tau_{p0})^{1/2} n_i \exp[qV_a/2kT],$$

$$p(x_m) = (\tau_{p0}/\tau_{n0})^{1/2} n_i \exp[qV_a/2kT]. \tag{7}$$

Since the carrier concentrations at any two points, x_a and x_b, are related by the electrostatic potential difference,[24]

$$n(x_a)/n(x_b) = \exp\{q[\psi(x_a) - \psi(x_b)]/(kT)\}, \tag{8}$$

we may now express the recombination rate as a function of the potential difference from the point of maximum recombination rate, x_m:

$$U(\Delta\psi) = \frac{n_i^2\{\exp[qV_a/(kT)-1]\}}{\tau_{n0}p(x_m)\exp[-q\Delta\psi/(kT)] + \tau_{p0}n(x_m)\exp[q\Delta\psi/(kT)] + \tau_{n0}p_1 + \tau_{p0}n_1}$$

$$= n_i\sinh[qV_a/(2kT)]\{(\tau_{n0}\tau_{p0})^{1/2}(\cosh[q\Delta\psi/(kT)] + \beta)\}^{-1}, \tag{9}$$

where[20]

$$\beta = [n_1(\tau_{p0}/\tau_{n0})^{1/2} + p_1(\tau_{n0}/\tau_{p0})^{1/2}]$$
$$\times \{2n_i \exp[qV_a/(2kT)]\}^{-1} \quad (10)$$

and $\Delta\psi = \psi(x) - \psi(x_m)$. In our previous work,[21] a value of zero was assumed for β in Eq. (9). The potential can be expanded as a power series about its value at x_m. Since we assume in this section that the recombination rate is strongly peaked[11] around x_m, a good approximation to recombination rates near the maximum may be obtained by retaining only the linear term of this expansion.[12] This amounts to assuming a constant value of electrostatic field[11] equal to its value at x_m, corresponding to the following linear approximation for the potential variation,

$$\Delta\psi(x) = F(x_m)\Delta x, \quad (11)$$

where $\Delta x = x - x_m$. If we assume that x_m is on the p-type side of the metallurgical junction then the field at the point of maximum recombination is given by (see Appendix B)

$$F(x_m) = ((2kT/\epsilon)\{N_A \ln[p_{p,\text{bulk}}/p(x_m)] - p_{p,\text{bulk}}$$
$$+ p(x_m) - n_{p,\text{bulk}} + n(x_m)\})^{1/2}, \quad (12)$$

where $p_{p,\text{bulk}}$ and $n_{p,\text{bulk}}$ are the carrier concentrations at the edge of the p-type bulk region (see Appendix B). The expression given by Choo[13] for the field at x_m is identical if we exchange N_A for N_D and invert the ratio of lifetime parameters. These changes merely allows for our assumption that x_m is on the p-type side of the junction since Choo assumes the opposite case.

We may now integrate $U(x)$ according to Eq. (3). Since the recombination rate is strongly peaked near the maximum, the results of the integration do not strongly depend on the boundaries to the integration. Hence, we extend the limits of integration to $\pm\infty$ in order to obtain an analytical solution. As we shall show, the consequences of this assumption are not serious enough to prevent us from obtaining a more accurate solution than by "standard" techniques[1,3] for many realistic situations. Equation (3) becomes, under our assumptions,

$$J_{rg}(1) \approx q \int_{-\infty}^{\infty} U \, dx$$
$$\approx 2qL_E n_i \sinh[qV_a/(2kT)](\tau_{n0}/\tau_{p0})^{-1/2}$$
$$\times \int_0^{\infty} (\cosh u + \beta)^{-1} du, \quad (13)$$

where $u = \Delta x/L_E$, $L_E = kT/[qF(x_m)]$, and $\Delta x = x - x_m$. The integral may be solved analytically using a standard expression,[25]

$$\int_0^{\infty} \frac{du}{\beta + \cosh u} = 2(1-\beta^2)^{-1/2} \arctan[(1-\beta^2)^{1/2}$$
$$\times (1+\beta)^{-1}], \quad \beta^2 < 1$$
$$= (\beta^2-1)^{-1/2} \ln\{[\beta+1+(\beta^2-1)^{1/2}]$$
$$\times [\beta+1-(\beta^2-1)^{1/2}]^{-1}\}, \quad \beta^2 > 1. \quad (14)$$

B. Cases where $U(x)$ is step-like

For the situations shown in Fig. 1 to result in $U(x)$ functions which are not strongly peaked but are, instead, step-like, the integration between infinite limits in Eq. (14) is inappropriate since it will result in an over-estimation of the recombination current. This situation occurs for large lifetime asymmetries at low voltages and moderate asymmetries for higher voltages. If $\tau_{n0} \ll \tau_{p0}$, as has been assumed here, then $\tau_{p0}(n+n_1)$ may be the dominant term in the denominator of Eq. (1). Then,

$$U \approx n_i^2\{\exp[qV_a/(kT)]-1\}[\tau_{p0}(n+n_1)]^{-1}. \quad (15)$$

We approximate the integral of Eq. (3) by "squaring off" the actual $U(x)$ function (see curves for which $\tau_{n0} \ll \tau_{p0}$ in Fig. 1) so that it is described by Eq. (15) between the edge of the p-type bulk and some point, $x(n=n^*)$, and by zero elsewhere. We call the range of Eq. (15), Δx^*. In order to make such an approximation it is necessary to assume some constant value for the minority carrier concentration, n, throughout the region where U is significant. We use $n = n_{p,\text{bulk}}$ [see Eq. (B12)]. The value of n^* is found by solving Eq. (15) for n when U is equal to the arithmetic mean of the recombination rates in the two bulk regions,

$$U_{\text{mean}} = 0.5\tau_{p0}^{-1}[N_D^{-1} + n_{p,\text{bulk}}^{-1}]n_i^2\{\exp[qV_a/(kT)]-1\}, \quad (16)$$

where majority bulk electron concentration has been approximated by the doping density, N_D. Hence, n^* is given by

$$n^* = \{\exp[qV_a/(kT)]-1\}(U_{\text{mean}}\tau_{p0})^{-1} - n_1. \quad (17)$$

In order to find Δx^*, the range over which Eq. (15) is assumed to be valid, we first find the potential difference across the range from Eq. (8),

$$\Delta\psi = kT/q \, \ln(n^*/n_{p,\text{bulk}}). \quad (18)$$

Under the assumption of quadratic spatial variation of potential which follows from the depletion approximation[26] applied over the region of interest, we have the following expression for Δx^*:

$$\Delta x^* \approx [2\Delta\psi\epsilon/(qN_A)]^{1/2} \quad (19)$$

and

$$J_{rg}(2) \approx qn_i^2\{\exp[qV_a/(kT)]-1\}$$
$$\times \Delta x^*[\tau_{p0}(n_{p,\text{bulk}}+n_1)]^{-1}. \quad (20)$$

C. Overall solution

Our final estimate for the recombination current is found by artificially combining the two expressions for $J_{rg}(1)$ and $J_{rg}(2)$:

$$J_{rg}^{-1} = J_{rg}^{-1}(1) + J_{rg}^{-1}(2). \quad (21)$$

Figure 3 shows J_{rg}, $J_{rg}(1)$, and $J_{rg}(2)$ as functions of lifetime asymmetry for a symmetrically doped junction at 0.2 V forward bias. The current, J_{rg}, is approximated by $J_{rg}(1)$ for small differences in the lifetimes and by $J_{rg}(2)$ when $\tau_{n0} \ll \tau_{p0}$.
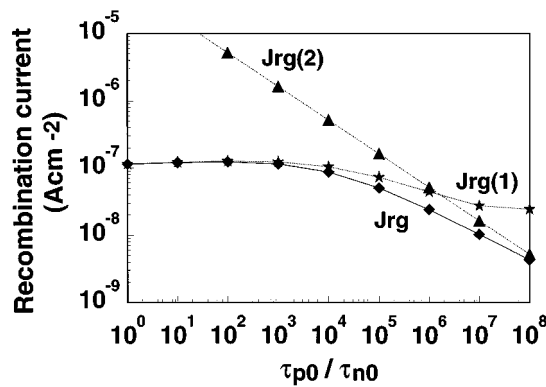
R. Corkish and M. A. Green

FIG. 3. Components of the junction recombination current according to the model presented in this work. The recombination current is approximated by $J_{rg}(1)$ when the lifetime asymmetry is small and by $J_{rg}(2)$ when it is large. The results were calculated by assuming $\tau_{p0}\tau_{n0}=10^{-12}$ s^2, $N_A=N_D=10^{16}$ cm^{-3}, $E_t=E_i$, and forward bias of 0.2 V.

IV. MODELING RECOMBINATION CURRENT USING PC-1D

For the PC-1D modeling we used the silicon data set and all surface recombination velocities were set equal to zero. This affects bulk current components but not depletion region current. Each side of the junction was described as a separate region.[18] Our PC-1D current values are estimated from the differences in current across the SCR [as defined by Eq. (4)] from the PC-1D output curves of current versus position. We used linear interpolation between the sample points provided by the program. The values of current found in this way show some variation with the overall thickness of the device (i.e., with the extent of the bulk regions included) in the finite element analysis. All the PC-1D results presented in this work were found using overall device thicknesses equal to $10W_n+10W_p$ except where this strategy would result in either side being thinner than 0.1 μm, which is ten times the default grading layer between regions.[18] In such cases the thickness of that side of the diode was set to 0.1 μm.

The PC-1D model includes band-gap narrowing which results from doping heavier than defined thresholds. Any further doping increase causes a reduction in the effective band gap in proportion to the natural logarithm of the doping density.[27] The thresholds used here are 7×10^{17} cm^{-3} for donors and 1×10^{17} cm^{-3} for acceptors. This explains the different height of one of the peaks in Fig. 2(b). None of the analytical models includes band-gap-narrowing effects.

V. RESULTS AND DISCUSSION

A. Lifetime asymmetry

1. Recombination centers at the intrinsic energy level, E_i

The results for lifetime (parameter) asymmetry from the various models and from the finite element analysis are compared in Fig. 4. A junction forward bias of 0.4 V and equal doping densities of 10^{16} cm^{-3} have been assumed. As the ratio of the hole and electron lifetimes was varied, their product was maintained constant, $\tau_{n0}\times\tau_{p0}=10^{-12}$ s. Our present
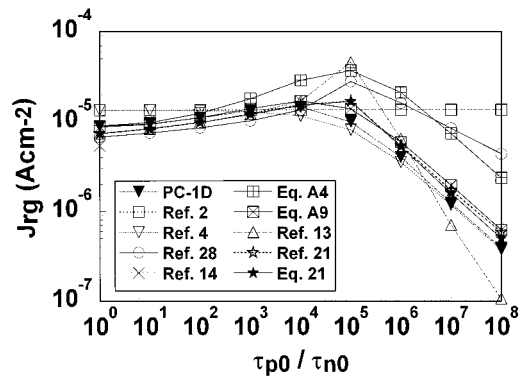

FIG. 4. Depletion-region recombination current as a function of lifetime asymmetry. Trap energy is equal to the intrinsic energy, forward bias is 0.4 V and the product of the lifetime parameters, $\tau_{p0}\tau_{n0}$, is set to 10^{-12} s^2.

and earlier[21] models achieve good agreement with PC-1D throughout the range of lifetime asymmetry. Simeonov and Ivanovich[28] have good agreement with PC-1D for asymmetry $\leq 10^4$. The SNS and (original) Choo[3] models both overestimate the current by a factor ~ 2 for low asymmetry and SNS grossly overestimate at high asymmetry. Choo's modified model[13] agrees well with the numerical calculations for small asymmetry but not when $\tau_{p0}/\tau_{n0}>10^4$. Only one point calculated from Shur's[14] expression has been included in Fig. 4 since that work is based on the assumption of equal lifetimes. Nussbaum's method [see Eq. (A4)] overestimates the current (as we have defined it here) when the asymmetry is enough to cause $U(x)$ to become step-like since significant additional bulk recombination is then included. The modified version of Nussbaum's method [see Eq. (A9)] is in excellent agreement with PC-1D throughout.

2. Recombination centers' energy level not at E_i

Our previous model[21] was based on the assumption that the trap energy is close to the intrinsic energy but that simplification is not necessary. Figure 5 shows the results, as a function of lifetime asymmetry, from the various models $E_t-E_i=-10kT$. The doping is assumed to be symmetrical, and the forward voltage is set to 0.4 V. Our previous work,
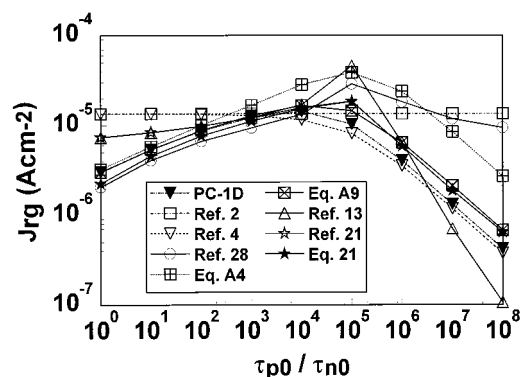

FIG. 5. Depletion-region recombination current as a function of lifetime asymmetry. Trap energy is equal to E_i-10kT, forward bias is 0.4 V and the product of the lifetime parameters, $\tau_{p0}\tau_{n0}$, is set to 10^{-12} s^2.
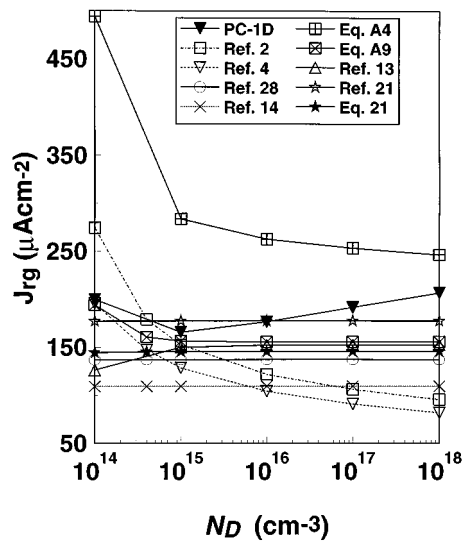
FIG. 6. Dependence of junction recombination current on doping asymmetry. The acceptor doping is kept at 10^{14} cm^{-3} while the donor doping on the opposite side of the junction is varied. The chosen range ensures that most of the recombination occurs on the p-type side of the junction. The carriers have equal lifetime parameters, $\tau_{p0} = \tau_{n0} = 10^{-6}$ s and the forward bias is 0.4 V.
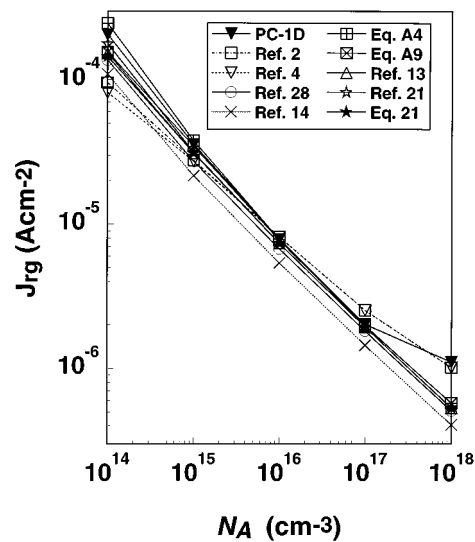
FIG. 7. Dependence of junction recombination current on doping asymmetry. The donor doping is kept at 10^{18} cm^{-3} while the acceptor doping on the opposite side of the junction is varied. The chosen range ensures that most of the recombination occurs on the p-type side of the junction. The carriers have equal lifetime parameters, $\tau_{p0} = \tau_{n0} = 10^{-6}$ s and the forward bias is 0.4 V.

along with the SNS and both Choo models, seriously overestimates the current when the lifetime asymmetry is small. The error exceeds an order of magnitude at a bias of 0.2 V. Choo's recent model gives poor agreement for high asymmetry but the original Choo work agrees well with PC-1D in that region. Nussbaum tends to overestimate the current when the form of $U(x)$ becomes step-like. Both our present formulation and the modified form of Nussbaum's give reasonable agreement with PC-1D throughout the range.

B. Doping asymmetry

We investigated the consequences of varying the doping on either the side of the junction on which x_m occurs or on the opposite side, while keeping the lifetime parameters fixed and equal. In these cases negligible error results from using $J_{rg}(1)$ in place of J_{rg}. For the curves shown in Fig. 6 the p-type doping is constant at $N_A = 10^{14}$ cm^{-3}, while the n-type doping density is varied over a range, $N_D \geqslant N_A$. This range ensures that the point of maximum recombination rate, x_m, remains on the p-type side of the junction. The modified form of Nussbaum's theory and our present and previous models each agree with the PC-1D results more closely than the other methods.

The other way to vary doping asymmetry is to keep the n-type doping density constant and vary the p-type doping over a range, $N_A < N_D$. Then x_m occurs on the same side of the junction as before. This method was used to obtain Fig. 7, for which the doping density on the n-type side was fixed at $N_D = 10^{18}$ cm^{-3}. Our methods, Nussbaum's method (unmodified or modified), and the recent Choo method produce results which are closer to those from PC-1D than are those from SNS or Choo (original model) for most of the range. The agreement of SNS and Choo[3] with the PC-1D results for $N_A = 10^{18}$ cm^{-3} is a fortuitous result of the band-gap

narrowing model in PC-1D. If band-gap narrowing had been excluded, as it was from the analytical models, the PC-1D result would have been reduced to 331.4 nA cm^{-2}.

VI. CONCLUSIONS

We have shown that significant errors (relative to the PC-1D finite element analysis with the SCR defined according to the depletion approximation) in the estimation of junction recombination currents under forward bias by other models may be reduced in many important cases by the use of a new analytical model which does not require numerical integration. When the excess carrier lifetime parameters are not highly asymmetrical only one of the two parts of the model [Eq. (13)] is required and that expression avoids reliance on the depletion approximation. When the lifetime parameters are highly asymmetrical it is necessary to apply a correction term [Eq. (20)]. Together [Eq. (21)], the two expressions provide an excellent description of the forward-bias recombination current across the SCR as defined by the depletion approximation. However, it should be noted that the depletion approximation is not always a good model for the extent of the SCR when the doping is asymmetrical. In addition we have demonstrated that Nussbaum's model may be brought into excellent agreement with a finite-element analysis by a simple variation of the limits of integration which prevent the inclusion of bulk recombination in the calculation of space-charge region recombination current.

APPENDIX A: ALTERNATIVE DERIVATION AND MODIFICATION OF NUSSBAUM'S METHOD

We give an alternative derivation of Nussbaum's method[16] of integrating the recombination current with respect to potential rather than distance and demonstrate how the limits of integration may be adjusted to achieve agreement with results from PC-1D using the spatial limits of Eq. (4).

From Eq. (3) we see that

$$dJ = qU \, dx. \tag{A1}$$

Multiplying each side by $F = -d\psi/dx$, where F is the field intensity, yields

$$F \, dJ = qU \, d\psi \tag{A2}$$

and integration of both sides allows the current change to be expressed in terms of an integral with respect to potential,

$$\int_{J_0}^{J_W} dJ = q \int_{\psi_0}^{\psi_W} (U/F) d\psi, \tag{A3}$$

where ψ_0 and ψ_W refer to the limiting values of potential in the p-type and n-type bulk regions, respectively. The limits, J_0 and J_W, designate the currents at the locations where those potential limits are reached, ie. where $F \to 0$. The integral on the right-hand side of Eq. (A3) must be divided into two parts since the field is differently defined on each side of the junction,

$$J_{rg} = J_W - J_0 = q \left[\int_{\psi_0}^{\psi_J} (U/F_p) d\psi + \int_{\psi_J}^{\psi_W} (U/F_n) d\psi \right], \tag{A4}$$

where ψ_J is the potential at the junction.

Choosing $\psi_0 = 0$ implies that

$$\psi_W = V_{bi} - V_a = kT/q \, \ln(n_n p_p / n_i^2) - V_a, \tag{A5}$$

where n_n and p_p are the (position-independent) majority-carrier densities in the bulk regions. From the derivation in Appendix B we have expressions for the field on either side of the junction,

$$F_p^2(x) = 2/\epsilon \{ kT[p(x) - p_p + n(x) - n_p] + qN_A\psi(x) \} \tag{A6}$$

and

$$-F_n^2(x) = 2/\epsilon \{ kT[p_n - p(x) + n_n - n(x)] + qN_D[\psi(x) - \psi_W] \}. \tag{A7}$$

By adding Eqs. (A6) and (A7) at the junction, where $F_p = F_n$, a solution is found for the junction potential,

$$\psi_J = \psi_W N_D (N_A + N_D)^{-1} - kT/q(n_n - n_p + p_n - p_p) / (N_A + N_D). \tag{A8}$$

Expressions for the carrier concentrations on the p-type side of the junction are given in Eqs. (B11) and (B12) and those for the other side may be found similarly. This allows Eq. (A4) to be solved.

Since the limits of the integrals in Eq. (A3) are defined by the field decreasing to zero, the corresponding positions lie beyond the SCR as defined by the depletion approxima-

tion. Hence, this method tends to give values for the recombination current which exceed those produced by the other methods, especially when the recombination rate in either bulk region is comparable to or exceeds that in the SCR. We have found by trial and error that this method may be modified to give agreement with PC-1D by adjusting the potential limit at each extreme by $\alpha = 0.3kT$. This results in the following expression for the recombination current to replace Eq. (A4),

$$J_{rg} = q \left[\int_{\alpha}^{\psi_J} (U/F_p) d\psi + \int_{\psi_J}^{\psi_W - \alpha} (U/F_n) d\psi \right]. \tag{A9}$$

APPENDIX B: ELECTRIC FIELD IN THE SPACE-CHARGE REGION

Here we derive Eq. (12), the expression for the electrostatic field amplitude at some point within the SCR where the charge density is known although the location of the point relative to the metallurgical junction may be unknown. A similar expression has previously been used by Green[29] and was based on work by Sparkes[30] and Green and Shewchun.[31]

We begin with Poisson's equation,

$$\frac{dF(x)}{dx} = \frac{\rho(x)}{\epsilon} = \frac{q}{\epsilon} [p(x) - n(x) + N_D(x) - N_A(x)], \tag{B1}$$

where $\rho(x)$ is the space-charge density at x, ϵ is the dielectric constant, and $N_D(x)$ and $N_A(x)$ are the ionized donor and acceptor concentrations at x. Rearranging and multiplying through by $F(x)$ and we find

$$\int F(x)dF = q/\epsilon \left\{ \int p(x)F(x)dx - \int n(x)F(x)dx \right. \\ \left. + \int [N_D(x) - N_A(x)]F(x)dx \right\}. \tag{B2}$$

Now, since the hole and electron currents are the sum of their drift and diffusion components,

$$J_p(x) = q\mu_p p(x)F(x) - kT\mu_p \, dp/dx, \\ J_n(x) = q\mu_n n(x)F(x) + kT\mu_n \, dn/dx, \tag{B3}$$

where μ indicates mobility, it is possible to derive expressions for the first two terms on the right-hand side of Eq. (B2):

$$\int p(x)F(x)dx = (q\mu_p)^{-1} \int J_p \, dx + kT/q \int dp, \\ \int n(x)F(x)dx = (q\mu_n)^{-1} \int J_n \, dx - kT/q \int dn. \tag{B4}$$

Substitution of Eq. (B4) into Eq. (B2) yields

$$\int F(x)dF = kT\epsilon^{-1} \left(\int dp + \int dn \right) - q\epsilon^{-1} \int [N_D(x) - N_A(x)]d\psi - \epsilon^{-1} \int (J_n/\mu_n - J_p/\mu_p)dx, \tag{B5}$$

J. Appl. Phys., Vol. 80, No. 5, 1 September 1996

R. Corkish and M. A. Green   3089

where $d\psi = -F(x)dx$. Green and Shewchun[31] found that the current integral may be neglected for typical silicon devices if the current does not exceed 1 A/cm^2. Integration allows us to find the difference in the square of the electric field between two points, x_a and x_b, in terms of the carrier concentrations and potential values at those points. The position of the points may be unknown. Hence,

$$F_b^2 - F_a^2 = 2kT\epsilon^{-1}(p_b - p_a + n_b - n_a) - 2q\epsilon^{-1}$$
$$\times [(N_{Db} - N_{Ab})\psi_b - (N_{Da} - N_{Aa})\psi_a], \quad (B6)$$

where the subscripts refer to the two points under consideration. We now assume that x_b is situated within the p-type bulk region far from the junction and that x_a is in the SCR on the p-type side of the abrupt junction. We therefore assume that at each point, $N_A \gg N_D$ and that $N_{Aa} = N_{Ab} = N_A$. The assumption of constant quasi-Fermi levels allows us to express the potential difference between the two points in terms of the hole concentrations,

$$\psi_b - \psi_a = kT/q \ \ln(p_a/p_b), \quad (B7)$$

and we set $F_b = 0$ since x_b is far from the junction. These assumptions result in the following expression for the field at x_a:

$$F_a^2 = 2kT\epsilon^{-1}[N_A \ \ln(p_b/p_a) - p_b + p_a - n_b + n_a], \quad (B8)$$

which is equivalent to Eq. (12) in the text.

In order to find values for the carrier concentrations in the p-type bulk region, we assume the space charge to be zero,

$$p_b - n_b - N_A = 0, \quad (B9)$$

and apply Eq. (6), so that

$$p_b = n_i^2 \ \exp[qV_a/(kT)]/n_b. \quad (B10)$$

Solving Eqs. (B9) and (B10) simultaneously yields expressions for the bulk concentrations:

$$p_b = 0.5(N_A + \{N_A^2 + 4n_i^2 \ \exp[qV_a/(kT)]\}^{1/2}), \quad (B11)$$

$$n_b = n_i^2 \ \exp[qV_a/(kT)]/p_b. \quad (B12)$$

If we were to make the additional assumptions that $p \gg n$ at each point of interest and that $p_b \approx N_A$ we would have the expression given by Green:[29]

$$F_a^2 = 2kT\epsilon^{-1}[N_A \ \ln(N_A/p_a) - N_A + p_a]. \quad (B13)$$

However, Eqs. (B8), (B11), and (B12), rather than Eq. (B13), were used for the calculations in this work.

[1] C.-T. Sah, R. N. Noyce, and W. Shockley, Proc. IRE **45**, 1228 (1957).
[2] See Eq. (27) of Ref. 1.
[3] S. C. Choo, Solid-State Electron. **11**, 1069 (1968).
[4] See Eq. (13) of Ref. 3.
[5] R. N. Hall, Phys. Rev. **87**, 387 (1952); W. Shockley and W. T. Read, Jr., *ibid*. **87**, 835 (1952).
[6] The excess carrier lifetime parameters, τ_{n0}, τ_{p0}, are equal to the excess carrier lifetimes, τ_n, τ_p, only for extrinsic material in low-level injection when the density of recombination centers is small and there is only a small deviation from thermal equilibrium. These conditions are discussed by C.-T. Sah, *Fundamentals of Solid-State Electronics* (World Scientific, Singapore, 1991), pp. 294–295. The lifetime parameters are not simply related to the lifetimes in a space-charge region.
[7] W. Shockley, Bell Syst. Tech. J. **28**, 435 (1949).
[8] M. A. Green, MSc thesis, University of Queensland, 1971, pp. 31–34; A. Nussbaum, Semicond. Semimet. **15**, 39 (1981), Fig. 5.
[9] See part III and especially Eq. (15) of Ref. 1.
[10] A. van der Ziel, *Solid State Physical Electronics*, 3rd ed. (Prentice–Hall, Englewood Cliffs, NJ, 1976), pp. 332–334.
[11] S. S. Simeonov and M. D. Ivanovich, Phys. Status Solidi A **82**, 275 (1984).
[12] C. D. Parikh and F. A. Lindholm, IEEE Trans. Electron Devices **ED-39**, 2197 (1992).
[13] S. C. Choo, Solid-State Electron. **39**, 308 (1996).
[14] M. Shur, IEEE Trans. Electron Devices **ED-35**, 1564 (1988).
[15] V. I. Starosel'skii, Russian Microelectron. **23**, 92 (1994).
[16] A. Nussbaum, Phys. Status Solidi A **19**, 441 (1973); Semicond. Semimet. **15**, 39 (1981), Eq. (170).
[17] J. P. McKelvey, *Solid State and Semiconductor Physics* (Harper and Row, New York, 1966), p. 403.
[18] P. A. Basore, PC-1D Installation Manual and User's Guide Version 3, Sandia National Laboratories Report No. SAND91-0516, 1991 (revised).
[19] A. Schenk, J. Appl. Phys. **71**, 3339 (1992); G. A. M. Hurkx, D. B. M. Klaassen, and M. P. G. Knuvers, IEEE Trans. Electron Devices **ED-39**, 331 (1992); J. Piprek and A. Schenk, J. Appl. Phys. **73**, 456 (1993); Stephen Robinson, Ph.D. thesis, University of New South Wales, 1995.
[20] M. A. Green, *Silicon Solar Cells, Advanced Principles and Practice* (Bridge Printery, Sydney, 1995), p. 305.
[21] R. Corkish and M. A. Green, *Solar '95*, Proceedings of the Annual Conference of the Australian and New Zealand Solar Energy Society, 1995, Hobart (ISBN 0 85901 6358), p. 93.
[22] S. J. Robinson, A. G. Aberle, and M. A. Green, IEEE Trans. Electron Devices **ED-41**, 1556 (1994).
[23] M. A. Green, *Silicon Solar Cells. Advanced Principles and Practice* (Bridge Printery, Sydney, 1995), pp. 340–341.
[24] See, for example, C.-T. Sah, *Fundamentals of Solid-State Electronics* (World Scientific, Singapore, 1991), pp. 262–265.
[25] I. S. Gradshteyn and I. M. Ryzhik, *Table of Integrals, Series and Products*, 5th ed. (Academic, Boston and London, 1994), p. 389, Item 3.513.2.
[26] See, for example, G. W. Neudeck, *The PN Junction Diode*, 2nd ed. (Addison–Wesley, Reading, MA, 1989), p. 32.
[27] Ref. 18, p. 22.
[28] See Ref. 11, Eqs. (9) and (10). For consistency with the other methods, N_d was replaced by N_A in Eq. (4) of Ref. 11 and in the expression for "B" following Eq. (6) in Ref. 11 and the lifetime ratio was inverted. This had the effect of ensuring that x_m was located on the p-type side of the junction rather than the n-type side as was assumed in Ref. 11.
[29] M. A. Green, J. Appl. Phys. **47**, 547 (1976); Solid-State Electron. **21**, 1139 (1978).
[30] J. J. Sparkes, J. Electron. Control **16**, 153 (1964).
[31] M. A. Green and J. Shewchun, Solid-State Electron. **17**, 349 (1974), Appendix B, Part (b).